INTERNATIONAL JOURNAL FOR NUMERICAL METHODS IN FLUIDS, VOL. 26, 177–197 (1998)

AN APPROACH FOR UNSTEADY LIFTING-LINE TIME-MARCHING NUMERICAL COMPUTATION

PH. DEVINANT

Laboratoire de Mécanique et d'Energétique, Ecole Supérieure de l'Energie et des Matériaux, Université d'Orléans, Rue Léonard de Vinci, F-45072 Orléans Cedex 2, France

SUMMARY

This paper presents the basis of a computational time-marching approach, for large-aspect ratio lifting systems submitted to unsteady motions, using the lifting-line concept. When engineering requires such an approach, quasi-steady ones are currently encountered, which are based on Prandtl's lifting-line approach for steady flows. The results of recent theoretical works on the unsteady lifting-line, based on the matched asymptotic expansion technique, allow one to improve, on sound theoretical foundations, this quasi-steady approach. The proposed approach solves a first-order approximation of the unsteady outer problem for the time-evolution of the spanwise circulation distribution along the lifting-line. It introduces, in the same kind of process as Prandtl's one, for each span section, an unsteady two-dimensional description of the aerofoil behaviour together with a formulation for the three-dimensional unsteady induced velocity on the lifting-line. The approach's validity is examined through a simple numerical implementation for three wing motion cases. Considering the numerical results it produces, it can be stated that the unsteady lifting-line model implementation can be considered as time-consistent, whereas the quasi-steady one cannot. Furthermore, the approach presented here allows large time steps, even for very unsteady wing motions, and compares favourably with some classical results of R. T. Jones. © 1998 John Wiley & Sons, Ltd.

Int. J. Numer. Meth. Fluids, **26**: 177–197 (1998)

KEY WORDS: unsteady flow; lifting-line; numerical computation

1. INTRODUCTION

The development of computational fluid dynamics techniques, together with the development of computer facilities, allows numerical simulations of increasingly complex flows. Nevertheless, sophisticated numerical approaches such as those based on the discretization of the Euler/Navier–Stokes equations, increasingly efficient though they are, often do not provide a clear qualitative understanding of the physical phenomena involved, whereas such an understanding, which is most important for engineering purposes, can be achieved through an asymptotic approach.

One of the most widespread asymptotic approaches as far as aerodynamics is concerned is the lifting-line model for large-aspect-ratio lifting systems ($AR = b/c \gg 1$, where b is the span length scale and c is the chord length scale) at subsonic speed.

Correspondence to: Ph. Devinant, Laboratoire de Mécanique et d'Energétique, Ecole Supérieure de l'Energie et des Matériaux, Université d'Orléans, Rue Léonard de Vinci, F-45072 Orléans Cedex 2, France. Email: Philippe.Devinant@univ-orleans.fr

CCC 0271–2091/98/020177–21 $17.50 *Received June 1996*

The steady lifting-line model, as introduced by Prandtl, is obtained by considering a two-dimensional problem in each span section, where the finite aspect ratio of the wing is accounted for via an induced incidence, and leads to the integral equation that governs the spanwise circulation distribution. Van Dyke[1] (see also References 2 and 3) has exhibited the singular perturbation characteristic of this problem once linearized and, with the help of the matched asymptotic expansion (MAE) technique, elaborated an asymptotic solution in the case of steady flows for unswept wings. This, particularly, justifies Prandtl's approach as a first-order approximation for the outer problem, using Van Dyke's terminology. An important feature of this concept is its unrivalled ease and flexibility of implementation, particularly when the computation time and resources are critical constraints (design cycles including many configuration investigations, quasi-real-time simulation, etc.). This approach has led to many widely used computing applications, which very often extend the model from the theoretical framework in which is was elaborated (linearized steady flow for an unswept wing) to non-linear situations (cambered aerofoils, swept wings, free wake, etc.).

The theoretical efficiency of MAE methods induced, from the mid 1970s, several extensions to Van Dyke's basic theory, mainly in the cases of curved and swept wings and for unsteady flows. One can quote the works of James,[4] Van Holten,[5] Cheng,[6–8] Ahmadi and Widnall,[9] Guiraud and Slama[10] and more recently, the outstanding works of Guermond and Sellier,[11–13] who put forward a unified lifting-line theory for an arbitrary wing in harmonic motion through the whole spectral domain. Thus this rigorous theory can now be considered as achieved and complete, and its straightforward numerization provides invaluable results. Its applications are nevertheless restricted to the theoretical framework in which it has been elaborated, i.e. established periodic linearized movements of the wing.

As things are at present, as soon as engineering requires discrete time-marching unsteady lifting-line computations (helicopter rotor, wind turbines, air propellers, aerodynamics–structure coupling computations, etc.), one almost only meets what can be considered as quasi-steady models (see e.g. References 14 and 15). Practically, these approaches deal with the time evolution of the spanwise circulation distribution and are mere empirical extensions of the steady Prandtl lifting-line model, as they account for the unsteady three-dimensional wake issued from the trailing edge by a steady-type induced incidence effect and generally use steady aerofoil models which are sometimes replaced by more or less unsteady aerofoil behaviour schemes. As a matter of fact, if this is justified in the steady case, as shown by Van Dyke, it is not in the unsteady one.

The objective of this paper is thus to show that it is possible to elaborate, from the results of the theoretical developments mentioned above, a first-order approximation of the unsteady outer problem, which is actually an improvement of the quasi-steady approach. This then yields a numerical tool allowing one to compute the time evolution of the spanwise circulation distribution through a really unstationary time-marching lifting-line approach. This paper does not intend to be comprehensive on such a subject, as extensions of the basic approach presented here can easily be imagined, some of them being in progress, but has rather to be interpreted as a first approach to this problem.

A simple computation implementation, the aim of which is only to validate the present approach, has been devised on the same discretization basis for both quasi-steady and unsteady cases. A numerical investigation in the quasi-steady case shows that this approach cannot be considered as time-consistent as soon as unsteadiness is not negligible. Compared with the quasi-steady implementation, the unsteady one is built on the same algorithm, requires only a little programming effort and leads to only slight increases in computing time. On the other hand, this unsteady implementation settles the time consistency of the model and shows that significantly large computation time steps are allowable, even for very unsteady motions, which is of paramount importance for computation performances. Finally, the results are compared favourably with some classical results of R. T. Jones.

2. SOME RESULTS FROM UNSTEADY LIFTING-LINE THEORY

2.1. Introduction

The objective of this section is to present, in a very condensed manner, what we need from the unsteady lifting-line theory. Most of it comes from the paper by Guermond and Sellier,[13] which brilliantly synthesizes this problem, and after which writing anything valuable requires an exceptional mastery of this difficult subject. This is why the reading of that paper is recommended for a clear and comprehensive understanding of what follows, as well as for any theoretical justification.

This theory is built on a similar set of hypotheses as those leading to the steady lifting-line theory; that is, inviscid irrotational incompressible flow, around a thin large-aspect-ratio wing, submitted to small time-harmonic oscillations (heave, pitch, deformation, etc.) close to a rectilinear uniform translation, so that the wing and the wake issued from its trailing edge and extending to downstream infinity remain in the neighbourhood of the surface S and Σ respectively, both included in the (O, x, y) plane (see Figure 1). The wing and the wake are, in a classical manner, represented by vorticity distributions on the surfaces S and Σ respectively.

This problem involves three characteristic length scales, namely the chord length scale c, the wing span length scale b and the motion wavelength $\lambda = 2\pi U/\omega$, where U is the freestream velocity and ω is the oscillation radian frequency. Cheng has identified five frequency ranges in the case of high-aspect-ratio wings ($c \ll b$): very low frequencies ($c \ll b \ll \lambda$), low frequencies ($c \ll b = O(\lambda)$), intermediate frequencies ($c \ll \lambda \ll b$), high frequencies ($c = O(\lambda) \ll b$) and very high frequencies ($\lambda \ll c \ll b$).

The inner and outer asymptotic expansions are performed relative to the small parameter $\varepsilon = 1/AR = c/b$, as for the steady case.

2.2. Domain decomposition

Let $M(x, y)$ be a point of S. Following the approach using the MAE technique and described by Guermond and Sellier,[13] the influence of the vorticity distributions on S and Σ at the point M may be decomposed into that of the vortices located at distances of order c and that of the vortices located at distances of order b or larger. In the plane (O, x, y) the inner domain I is defined as the set of points whose distance from M is of order c. The diameter of I is set to an intermediate length scale d characterized by $c \ll d \ll b$. Two outer domains must be defined. The first one, denoted by O_{wi} is constituted of the points located in the wake of the inner domain at distances of order b or larger (see Figure 2). The width of O_{wi} is set to the intermediate reference scale d. The second outer domain,

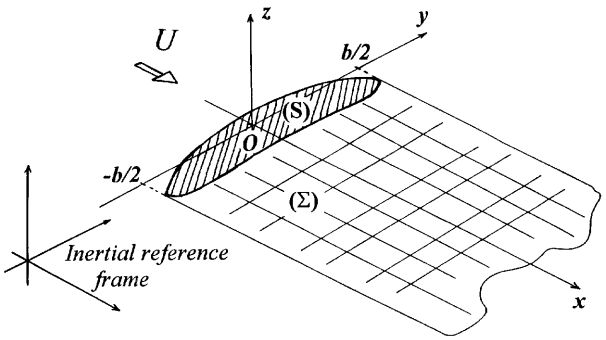

Figure 1. Three-dimensional unsteady linearized problem

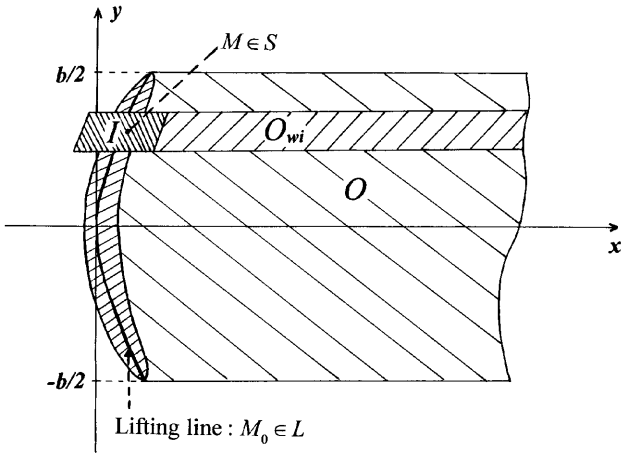

Figure 2. Domain decomposition

denoted by O, is composed of the points situated outside O_{wi} and at a distance from M of order b or larger (see Figure 2). The velocity induced at M by the vorticity distributions is the sum of the contributions of the three domains I, O_{wi} and O:

$$w(M) = w_{\mathrm{in}}(M) + w_{\mathrm{out}}(M),$$

where $w_{\mathrm{in}}(M)$ corresponds to the inner domain I and $w_{\mathrm{out}}(M)$ to the outer domain $O \cup O_{\mathrm{wi}}$.

2.3. Velocity induced by outer domain $O \cup O_{\mathrm{wi}}$

In the outer domain $O \cup O_{\mathrm{wi}}$ the reference length scale is b in both spanwise and streamwise directions. As a result, from this domain, the details of the geometry of the wing in the chordwise direction become insignificant; the wing degenerates into a line L, and M merges into $M_0 \in L$. For this outer domain the line L is a lifting-line as in Prandtl's model. It can then be shown that

$$w_{\mathrm{out}}(M) = \mathrm{e}^{-\mathrm{i}kx} w_{\mathrm{out}}(M_0),$$

where $w_{\mathrm{out}}(M_0)$ is the finite part (in Hadamard's sense) of the downwash induced at M_0 by the vorticity distributions of the outer domain $O \cup O_{\mathrm{wi}}$ (lifting-line and wake) and where $\mathrm{e}^{-\mathrm{i}kx}$, with the chord-reduced oscillation radian frequency $k = \omega c/U$, indicates a chord sinusoidal downwash modulation.

2.4. Velocity induced by O_{wi}

In the domain O_{wi}, the length scale in the spanwise direction is c, whereas b is the length scale in the streamwise one. The width of O_{wi} being of order d, at the first approximation order, O_{wi} may be considered as a two-dimensional semi-infinite vortex sheet whose upstream boundary matches the local tangent to L at M_0 and whose vorticity is aligned with this tangent. It can be shown that the downwash $w_{\mathrm{wi}}(M)$ induced at $M \in S$ by this vortex sheet reads, as for w_{out}

$$w_{\mathrm{wi}}(M) = \mathrm{e}^{-\mathrm{i}kx} w_{\mathrm{wi}}(M_0).$$

This term is important, as it means that spanwise flow perturbations of length scale of order c, which are generated in the inner domain I by the wing motion, are convected in the outer wake and are still active when they reach distances of order b and greater.

2.5. Velocity induced by inner domain I

In the inner domain, c is the common reference scale for both streamwise and spanwise directions and the diameter of I is of order d. This domain is composed of the wing section on which M is situated, together with its close wake. At the first order of approximation, only the component of vortices aligned with the local tangent to the lifting-line is of interest; furthermore, these vortices may be considered as constant in the spanwise direction. The downwash induced by these vortices may be decomposed into the downwash induced by the bound vortices (located on S), $w_{\text{bound}}(M)$, and that induced by the free vortices (located on the part of the wake Σ included in I), $w_{\text{free}}(M)$. Consequently, $w_{\text{bound}}(M)$ and $w_{\text{free}}(M)$ are two-dimensional contributions, but their sum is not the complete two-dimensional downwash $w_{2\text{D}}(M)$, because, however large the ratio d/c is, $w_{\text{free}}(M)$ will never include the influence of the vortices which have been convected out of I at distances of order b or larger. The vortices in question are those of O_{wi}. As a consequence, the exact two-dimensional downwash $w_{2\text{D}}(M)$ is the sum of $w_{\text{bound}}(M)$, $w_{\text{free}}(M)$ and $w_{\text{wi}}(M)$:

$$w_{2\text{D}}(M) = w_{\text{bound}}(M) + w_{\text{free}}(M) + w_{\text{wi}}(M).$$

2.6. First-order complete downwash

Finally, on the basis of the MAE technique the velocity field induced by the inner and outer vortex systems can be written to the first order of approximation as

$$w(M) = w_{2\text{D}}(M) + w_{\text{out}}(M) - w_{\text{wi}}(M) + o(1/AR). \tag{1}$$

The term $w_{\text{wi}}(M)$ has to be subtracted in (1), since it appears twice, once in $w_{2\text{D}}(M)$ and another time in $w_{\text{out}}(M)$.

3. AN APPROACH FOR TIME-MARCHING LIFTING-LINE COMPUTATION

The objective of the present section is to derive from the results presented in Section 2, and particularly from expression (1), a time-marching unsteady lifting-line computation method for the outer problem, exact to the first order of approximation.

3.1. Velocity field scheme

First of all, equation (1) can be rewritten to first order as

$$w(M) \approx w_{2\text{D}}(M) + w_{\text{i}}(M), \tag{2}$$

where, according to Prandtl's approach, $w_{2\text{D}}(M)$ corresponds to the normal perturbation velocity in the two-dimensional case (remaining when $AR \to \infty$) and $w_{\text{i}}(M)$ is customarily named the induced velocity, which represents the correction to this two-dimensional case due to the finite aspect ratio of the wing. As, from relation (1), $w_{\text{i}}(M) = w_{\text{out}}(M) - w_{\text{wi}}(M)$, this leads in the case of a straight unswept wing to the interpretation first put forward by Van Holten[5] and taken up again by Ahmadi and Widnall.[9] It may accordingly be stated that, to first order, the induced velocity field for a given point M of the wing, $w_i(M)$, is the difference between the velocities induced by two vortex systems relating respectively to $O \cup O_{\text{wi}}$ (i.e. w_{out}) and O_{wi} (i.e. w_{wi}). This is why an unsteady lifting-line model that considers only w_{out} and does not take w_{wi} into account (as most empirical models do) fails irremediably as soon as unsteadiness becomes significant.

Ahmadi and Widnall have also noticed that the induced velocity fields at any span station along the lifting-line for each of the vortex systems are logarithmically singular, but that their difference, which is precisely $w_i(M)$, no longer is.

It can of course be noticed that this result is a generalization of Prandtl's steady case approach for straight unswept wings. The steady induced velocity may be described in the same way: the wake corrresponding to $O \cup O_{wi}$ is free from unsteady aspects, the contribution of O_{wi} and the chord dependence vanish, and it is then possible to convert the constant induced velocity into an induced incidence, resulting from the composition of the freestream velocity U and this constant induced velocity.

Next the induced velocity field $w_i(M)$ may be written as

$$w_i(M) = w_i(M_0)e^{-ikx},$$

where

$$w_i(M_0) = w_{out}(M_0) - w_{wi}(M_0).$$

The chord-reduced oscillation frequency $k = \omega c/U$ has already been mentioned. Introducing the span-reduced oscillation frequency $\nu = \omega b/U$ and limiting the approach to low and very low frequencies ($b \ll \lambda$ or $b = O(\lambda)$), so that for high aspect ratios AR, $\nu = O(1)$, it can be seen that $k = \nu/AR = o(1)$; thus e^{-ikx} is only slightly different from unity and $w_i(M)$ is only slightly different from $w_i(M_0)$. Therefore, to first order, for low frequencies the chord sinusoidal downwash modulation will be neglected and $w_i(M)$ considered as constant along the chord. The generality of Guermond and Sellier's approach through the whole spectral domain is of course lost here, but this seems necessary, as will be seen later.

3.2. Basis for model formulation

It is now possible to suggest the principles of a first-order formulation for the unsteady lifting-line outer problem, based on the same kind of process as the one developed by Prandtl in the steady case.

As far as the outer problem is concerned, the wing reduces to the lifting-line L, and the only unknown at any instant t is the spanwise circulation distribution along this line, $\Gamma(y, t)$. Furthermore, the induced velocity field is considered as constant along the chords of the aerofoils constituting the wing: $w_i(M) = w_i(M_0)$, $M_0 \in L$. This *a priori* restricts the approach's validity to the low- and very-low frequency domains, as shown in Section 3.1; it may however be noticed that for classical engineering application such as those mentioned in Section 1, for which only low frequencies are of interest, this limitation is not really troublesome. On the other hand, this consistency is crucial as it allows one to adopt Prandtl's approach, since the three-dimensional aspect of the flow can be accounted for via an induced velocity w_i on the lifting-line.

Then the solution of the outer problem (the spanwise circulation distribution along the lifting-line L at the considered instant t, $\Gamma(y, t)$) will be sought through the resolution for each span station of the wing of a two-dimensional unsteady problem (corresponding to w_{2D} in (2)) that takes into account the finite aspect ratio of the wing via the induced velocity term $w_i(M_0)$ as defined in Section 3.1. Actually, this approach is quite comparable to Prandtl's one for the steady case, but it can be seen that an unsteady aerofoil behaviour description is required for each span section and that the concept of an induced velocity on the lifting-line does not have the same meaning.

Moreover, from Section 3.1 it is possible to settle the status of the quasi-steady approaches. As mentioned in Section 1, these approaches are empirical extensions of the steady Prandtl's lifting-line model and differ from the here-proposed unsteady process on two points. First, the two-dimensional problem generally involves a 2D steady aerofoil model (often issued from experiments, with Mach

and Reynolds number effects) instead of an unsteady one; it may also be noted[14] that empirical attempts have been made to introduce 2D unsteady models, including, in some cases, dynamic stall descriptions. Secondly, it accounts for the unsteady three-dimensional wake by a steady-type induced incidence based on the influence of the whole outer domain $O \cup O_{wi}$, omitting the negative contribution of O_{wi} in the induced velocity w_i on the lifting-line (and which actually does not exist in the steady case). It can therefore be said that any attempt to improve such an approach must take these two points into account.

4. MODEL FORMULATION

We will first examine in Section 4.1 the three-dimensional unsteady induced velocity $w_i(M_0)$. Then the formulation of the two-dimensional unsteady problem, based on a linearized unsteady aerofoil approach, will be considered in Section 4.2, for which the influence of the 2D far wake will partly combine with $w_i(M_0)$ and lead to the formulation of the problem exposed in Section 4.3.

In this paper the formulation is limited to straight unswept and rigid wings. This is not a theoretical limitation, and at present this formulation is in the process of extension to non-straight and swept wings.

4.1. Unsteady induced velocity

The results relating to the induced velocity scheme, as displayed in Section 2, rigorously apply to periodic established motions. It has to be assumed here that these results are still valid in the case of transient or non-established periodic motions. This hypothesis may be justified intuitively, arguing that such motions may always be regarded as part of a periodic installed movement, the period of which is large enough so that the wake shed during the previous periods has been convected far enough for its influence on the lifting-line (i.e. the velocity it induces) to become negligible.

The objective of this section is to derive from the above statements an expression for the unsteady induced velocity which will be used later on.

In the case of straight unswept wings the lifting line L is the segment

$$x = z = \text{constant} = 0 \quad -b/2 \leqslant y \leqslant b/2,$$

and the induced velocity on the lifting-line as defined in Section 3.2 varies along the span. It depends also on the considered instant t, as w_i is the velocity induced by the wake shed from the lifting-line whose geometry and spatial density distributions are time-dependent, according to the wing's unsteady motion and the wake's convection; thus

$$w_i(M_0) = w_i(y, t) = w_{out}(y, t) - w_{wi}(y, t). \tag{3}$$

The wing and the wake are represented, as already mentioned, by vorticity distributions on S and Σ respectively. The velocity induced at any point $P(x, y, z)$ by such distributions whose densities are $\gamma_x(\xi, \eta)$ in the x-direction and $\gamma_y(\xi, \eta)$ in the y-direction can be written classically (see e.g. Reference 16) as

$$w(x, y, z, t) = -\frac{1}{4\pi} \int_{S \cup \Sigma} \frac{\gamma_y(\xi, \eta)(x - \xi) + \gamma_x(\xi, \eta)(y - \eta)}{[(x - \xi)^2 + (y - \eta)^2 + z^2]^{3/2}} \, d\xi \, d\eta. \tag{4}$$

Then $w_{out}(y, t)$, corresponding to the outer domain $O \cup O_{wi}$, is the velocity induced on the lifting-line L by the lifting-line itself (S turns to L, and for a straight unswept wing this contribution is zero)

and the 3D vortex sheet (Σ turns to a 3D wake shed from the lifting-line L and extending to the downstream limit x_0) and can be written as

$$w_{\text{out}}(y,t) = -\frac{1}{4\pi}\,\text{FP}\int_{-b/2}^{b/2}\int_{0}^{x_0}\frac{\gamma_y(\xi,\eta)(-\xi)+\gamma_x(\xi,\eta)(y-\eta)}{[(-\xi)^2+(y-\eta)^2]^{3/2}}\,\mathrm{d}\xi\,\mathrm{d}\eta. \tag{5}$$

It is worth mentioning that the double integral in (5) is singular and has to be taken in the finite part (FP) sense as introduced by Hadamard (see Reference 13).

As stated in Section 2.4, $w_{\text{wi}}(y,t)$ is the velocity induced on the lifting-line by a semi-infinite two-dimensional vortex sheet whose upstream boundary is tangent to the lifting-line L and whose density then corresponds to the local value of $\gamma_y(\xi,\eta)$ for $\eta = y$, i.e. $\gamma_y(\xi,y)$, and can be written as

$$w_{\text{wi}}(y,t) = \frac{1}{2\pi}\,\text{FP}\int_{0}^{x_0}\frac{\gamma_y(\xi,y)}{\xi}\,\mathrm{d}\xi. \tag{6}$$

The integral in (6) is also singular and must also be taken in Hadamard's finite part sense.

Then the expression of the induced velocity on the lifting-line,

$$w_{\text{i}}(y,t) = w_{\text{out}}(y,t) - w_{\text{wi}}(y,t), \tag{7}$$

is obtained from (5) and (6).

The densities $\gamma_x(\xi,\eta)$ and $\gamma_y(\xi,\eta)$ in w_{out} and w_{wi} are related classically to the time and span variations of the circulation distribution $\Gamma(y,t)$. These are spatial densities, relating to the wake-describing co-ordinates (ξ,η), and their values are set once and for all when shed. Consider a vortex particle of the wake shed at the span location y and at time τ. In accordance with the linearized approach, its location at any later instant $t \geqslant \tau$ is $\xi = U(t-\tau)$, $\eta = y$ and the shedding corresponds to $\xi = 0$. Then, at instant $t = \tau$ its density $\gamma_y(0,y)$ is the time variation of $\Gamma(y,t)$ at the span location y, expressed as a streamwise variation with the help of the freestream velocity U, and $\gamma_x(0,y)$ corresponds to the span variation of $\Gamma(y,t)$ at the same instant and span location:

$$\gamma_y(0,y) = \frac{1}{U}\frac{\partial\Gamma(y,t)}{\partial t}, \qquad \gamma_x(0,y) = \frac{\partial\Gamma(y,t)}{\partial y}. \tag{8}$$

At any later instant $t \geqslant \tau$ these values are kept unchanged while the particle is convected with the freestream velocity:

$$\gamma_x(\xi,\eta) = \gamma_x(U(t-\tau),y), \qquad \gamma_y(\xi,\eta) = \gamma_y(U(t-\tau),y). \tag{9}$$

The induced downwash on the lifting-line defined by (5)–(7) is now ready to be incorporated in the two-dimensional model.

4.2. Two-dimensional problem

This two-dimensional problem, according to Section 3, deals for each span section, i.e. for each $y =$ constant plane, with the unsteady aerofoil theory. It is treated here within a linearized framework, as this choice is consistent with the theoretical 3D exposition and is thus preferred, but this is not compulsory and a non-linear one can be substituted.

This classical problem (see e.g. References 17–19) is presented in Figure 3. Couchet's notation and formulation are adopted. Each aerofoil of the lifting-line is considered as a rigid flat plate on the segment $[-2a,\ 2a]$ with a chord $c = 4a$. Its movement deduced from the lifting-line motion and considered in a motionless fluid, is defined by the velocity components of the aerofoil-attached frame relative to an inertial frame, $(l(t), m(t), q(t))$, expressed in the aerofoil-attached frame. Here $l(t)$

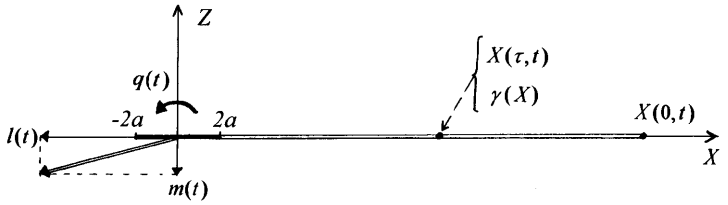

Figure 3. Two-dimensional linearized problem

represents the aerofoil longitudinal motion and it not very different from a rectilinear translatory motion l_0 (which is the opposite of the freestream velocity: $-U = l_0 < 0$), $m(t)$ is the vertical heave motion and $q(t)$ is the pitch motion around the aerofoil centre:

$$l(t) = l_0 + \tilde{l}(t), \qquad m(t) = \tilde{m}(t), \qquad q(t) = \tilde{q}(t),$$

where the linearization assumes that $\tilde{l}$, $\tilde{m}$ and $c\tilde{q}$ are small compared with l_0.

At time t the linearized wake on the OX-axis lies between the trailing edge at $X = 2a$ and the position at that time of the vortex particle shed at initial time $t = 0$, $X(0, t) = 2a - l_0 t$. Each vortex particle $X(\tau, t)$ is imparted the vortex density $\gamma(X)$, which is determined when shed at time $t = \tau$, and convected in the X-direction with velocity $-l_0$ relative to the aerofoil-attached frame: $X(\tau, t) = 2a - l_0(t - \tau)$. Particularly, $X(t, t) = 2a$ represents the particle being shed at the current instant t.

Then at instant t the set of equations describing this problem is

$$t \in [0, T]:$$

$$\frac{\partial \Gamma(t)}{\partial t} + l_0 \gamma(X(t, t)) = 0, \tag{10}$$

$$\Gamma(t) = -4\pi a(m + q\Omega) + \int_{2a}^{X(0,t)} \left[\sqrt{\left(\frac{\chi + 2a}{\chi - 2a} \right)} - 1 \right] \gamma(\chi)\, \mathrm{d}\chi, \tag{11}$$

with $\chi = \chi(\tau, t)$.

Equation (10) is obtained from Kelvin's theorem and expresses the circulation conservation; equation (11) is the integral equation, combining the tangency condition and the Kutta–Joukovski condition at the trailing edge, that governs the time evolution of the circulation $\Gamma(t)$ around the plate. The first term on the right-hand side of (11), where the dependence of m and q on t has been omitted, represents the aerofoil motion contribution (Ω is a characteristic length, equal to a in the case of a flat plate; the expression $q\Omega$ represents the rear quarter-chord point motion due to the pitch q)[19,20] and the second term gives the wake contribution.

It is possible to expand to first order for $\chi - 2a \gg a$ as

$$\sqrt{\left(\frac{\chi + 2a}{\chi - 2a} \right)} - 1 = \frac{2a}{\chi - 2a} + o\left(\frac{a}{\chi - 2a} \right). \tag{12}$$

Thus the kernel of the integral describing the wake contribution in (11) may be written to first order in $a/(\chi - 2a)$ as

$$\left[\sqrt{\left(\frac{\chi + 2a}{\chi - 2a} \right)} - 1 \right] \gamma(\chi) \approx \frac{2a}{\chi - 2a} \gamma(\chi) = 4\pi a \left(\frac{1}{2\pi} \frac{\gamma(\chi)}{\chi - 2a} \right) = 4\pi a k(\chi), \tag{13}$$

where accordingly $k(\chi)$ may be interpreted as the velocity at the trailing edge of the aerofoil induced by the vortex particle at position $X = \chi$ with density $\gamma(\chi)$.

Consequently, when writing the integral equation (11) describing the 2D unsteady problem, the above result allows us to represent the effect of the 2D far wake (i.e. for $\chi \gg a$) with an induced velocity field. Therefore it is possible to split the unsteady two-dimensional wake Σ_{2D} into two parts:

$$X' \gg a: \quad \Sigma_{2D} = [2a, X'] \cup [^{V'}, X(0, t)].$$

Hence the integral equation (11) reads

$$\Gamma(t) = -4\pi a(m + q\Omega) + \int_{2a}^{X'} \left[\sqrt{\left(\frac{\chi + 2a}{\chi - 2a} \right)} - 1 \right] \gamma(\chi)\, \mathrm{d}\chi + 4\pi a K, \tag{14}$$

with

$$K = \int_{X'}^{X(0,t)} k(\chi)\, \mathrm{d}\chi = \frac{1}{2\pi} \int_{X'}^{X(0,t)} \frac{\gamma(\chi)}{\chi - 2a}\, \mathrm{d}\chi. \tag{15}$$

4.3. General formulation of problem

The three-dimensional correction due to the induced velocity field as displayed in Section 4.1 must now complete the unsteady two-dimensional formulation presented in Section 4.2.

In the case of straight unswept wings the lifting-line is the segment

$$x = z = \text{constant} = 0, \quad -b/2 \leqslant y \leqslant b/2.$$

The aerofoil dimensional characteristics depend only on y according to the wing plan-form definition

$$c = c(y), \qquad a = a(y), \qquad \Omega = \Omega(y),$$

as do the aerofoil motion parameters

$$l(y, t) = l_0 + \tilde{l}(y, t), \qquad m(y, t) = \tilde{m}(y, t), \qquad q(y, t) = \tilde{q}(y, t),$$

which are deduced for each span station y from the wing motion parameters.

Then in each wing section the two-dimensional problem deals with the unknown circulation $\Gamma(y, t)$ at the considered section's span location y and time t. This problem is governed by a set of equations of the same kind as the set (10), (14) in Section 4.2, to which is added the reference to the considered section, y, and the effect of the induced velocity w_{i} (for simpler presentation the dependence of m, ω, Ω and a on y has been omitted; furthermore, $\gamma(\chi, y)$ refers to the two dimensional vortex density $\gamma(\chi)$, as introduced in Section 4.2, corresponding to the section's span location y):

$$y \in [-b/2, b/2], \quad t \in [0, T]:$$

$$\frac{\partial \Gamma(y, t)}{\partial t} + l_0 \gamma(X(\iota, t), y) = 0, \tag{16}$$

$$\Gamma(y, t) = -4\pi a(m + q\Omega) + \int_{2a}^{X'} \left[\sqrt{\left(\frac{\chi + 2a}{\chi - 2a} \right)} - 1 \right] \gamma(\chi, y)\, \mathrm{d}\chi + 4\pi a K(y, t) + F(y, t), \tag{17}$$

where $K(y, t)$ represents, according to (13), the velocity induced by the 2D far wake $[X', X(0, t)]$ in relation to the considered wing section y,

$$K(y, t) = \frac{1}{2\pi} \int_{X'}^{X(0,t)} \frac{\gamma(\chi, y)}{\chi - 2a}\, \mathrm{d}\chi,$$

and $F(y, t)$ represents the effect, for the considered section, of the induced velocity, w_i as developed in Section 4.1.

Then in the same manner as for the steady case a vertical induced velocity on the lifting-line, $w_i(y, t)$, may be represented by an opposite vertical movement in a motionless fluid, $m'(y, t)$, of the aerofoil located at this point, i.e. $m'(y, t) = -w_i(y, t)$, so that

$$F(y, t) = -4\pi a m'(y, t) = 4\pi a w_i(y, t),$$

where $w_i(y, t)$ is expressed by (7), in which $w_{out}(y, t)$ is obtained from (5) and $w_{wi}(y, t)$ from (4).

The contribution of $K(y, t)$ and $w_i(y, t)$ may then by introducing $W_i(y, t)$, be grouped together as

$$4\pi a K(y, t) + 4\pi a w_i(y, t) = 4\pi a(K(y, t) + w_i(y, t)) = 4\pi a W_i(y, t),$$

so that the integral equation (14) that governs the two-dimensional local problem can be written in the form

$$\Gamma(y, t) = -4\pi a(m + q\Omega) + \int_{2a}^{X'} \left[\sqrt{\left(\frac{\chi + 2a}{\chi - 2a} \right)} - 1 \right] \gamma(\chi, y)\, \mathrm{d}\chi + 4\pi a W_i(y, t). \tag{18}$$

Finally, $W_i(y, t)$ in (18) can be rearranged

$$W_i(y, t) = K(y, t) + w_i(y, t) = K(y, t) + w_{out}(y, t) - w_{wi}(y, t),$$

with

$$K(y, t) = \frac{1}{2\pi} \int_{X'}^{X(0,t)} \frac{\gamma(\chi, y)}{\chi - 2a}\, \mathrm{d}\chi, \qquad w_{wi}(y, t) = \frac{1}{2\pi} \mathrm{FP} \int_0^{x_0} \frac{\gamma_y(\xi, y)}{\xi}\, \mathrm{d}\xi,$$

where $K(y, t)$ corresponds to the 2D far wake in the 2D problem and $w_{wi}(y, t)$ corresponds to the 2D wake linked with the outer domain O_{wi}. It appears from Section 2 that both integrals relate to the same two-dimensional wake. In fact, it is possible to relate $K(y, t)$ and $w_{wi}(y, t)$ together through the variable change from $\chi - 2a$ to ξ. This means particularly that x_0 corresponds to $X(0, t)$ and that the two functions $\chi - 2a \to \gamma((\chi - 2a), y)$ and $\xi \to \gamma_y(\xi, y)$ are identical. Consequently, after having set $x' = X' - 2a \gg a$ and split the integral in $w_{wi}(y, t)$ into two parts as

$$w_{wi}(y, t) = \frac{1}{2\pi} \mathrm{FP} \int_0^{x'} \frac{\gamma_y(\xi, y)}{\xi}\, \mathrm{d}\xi + \frac{1}{2\pi} \int_{x'}^{x_0} \frac{\gamma_y(\xi, y)}{\xi}\, \mathrm{d}\xi \tag{19}$$

(the finite part concerns the integral's kernel singularity for $\xi = 0$, and so only the first integral in (19)), it can be seen that $K(y, t)$ is equal to the second term on the right-hand side of (19), such that $W_i(y, t)$ finally reads

$$W_i(y, t) = w_{out}(y, t) - \frac{1}{2\pi} \mathrm{FP} \int_0^{x'} \frac{\gamma_y(\xi, y)}{\xi}\, \mathrm{d}\xi. \tag{20}$$

In (20) the densities $\gamma_x(\xi, \eta)$ and $\gamma_y(\xi, \eta)$ appear, which are linked to the time and span variation of the distribution of circulation $\Gamma(y, t)$ by relations (8) and (9) in Section 4.1.

It is interesting to notice the following in equation (18).

1. The 2D model only concerns the near wake $[2a, X']$, as the contribution of the far wake $[X', X(0, t)]$ vanishes with part of the induced velocity.
2. $W_i(y, t)$, as defined in relation (20), appears as an 'effective induced velocity', which combines the effect on the lifting-line of the entire 3D wake ($w_{out}(y, t)$) with the effect of the nearer part of O_{wi}, $[0, x']$, which is a 2D-type one.

As a conclusion to this section, it can be stated that, for each instant t and span location y, equation (18), completed with relation (20), together with the vorticity conservation relation (16) and relations (8) and (9), builds up the intended unsteady lifting-line model, and its solution $\Gamma(y, t)$ is the solution to the first-order approximation of the outer (lifting-line) problem concerning the unsteady motion of a straight, unswept, large aspect-ratio wing.

This model is obtained from a linearized approach and is rigorously applicable only to that case. Nevertheless, it may be stated that, as the steady lifting-line model comes under the same linearization process and has been widely extended to non-linear situations (non-flat plate aerofoils, free wake, etc.), it is quite possible in the same manner to apply the unsteady lifting-line model described above to non-linear situations.

5. QUASI-STEADY APPROACH

At the same time as the above-evolved unsteady model, a quasi-steady-type model will be evaluated. This quasi-steady approach, already mentioned earlier, actually consists of applying Prandtl's steady case approach to an unsteady situation. This means that at each instant during the wing motion the two-dimensional model and the induced velocity scheme are steady-type ones. Actually, the quasi-steady model is included in the more general unsteady lifting-line one and will here be derived from it.

More precisely, the 2D model involves an expression obtained from (11) in Section 4.2, in which the term corresponding to the wake has been withdrawn, so that it becomes

$$\Gamma(t) = -4\pi a(m + q\Omega). \tag{21}$$

Most of the currently used quasi-steady models omit the term $q\Omega$, which represents the effect of the rotation of the profile, and only consider a translatory model; this presents the advantage that steady experimental aerofoil characteristics, with Mach number, Reynolds number, sweep effect and any other desired corrections, can be included. This is all the more an advantage since the induced velocity on the lifting-line is directly added to the 2D model described by equation (21) as an incidence correction effect. It will here be taken into account, in a quite equivalent manner, as an induced velocity that can be immediately obtained from relation (5) in Section 4.1:

$$W_{\mathrm{i}}^{QS}(y, t) = w_{\mathrm{out}}(y, t) = -\frac{1}{4\pi}\int_{-b/2}^{b/2}\int_{0}^{x_0} \frac{\gamma_y(\xi, \eta)(-\xi) + \gamma_x(\xi, \eta)(y - \eta)}{[(-\xi)^2 + (y - \eta)^2]^{3/2}}\, \mathrm{d}\xi\, \mathrm{d}\eta. \tag{22}$$

Most of, if not all, the quasi-steady models do not clearly consider the integral's singular behaviour and do not mention how it has to be evaluated. In fact, as these approaches are very often based on an already discretized vision of the problem, this singular aspect is evaded when using constant doublet panels, as will be seen later.

Finally, the considered quasi-steady approach can be summarized, using the same process and formalism as for the unsteady one, by the following relations:

$$y \in [-b/2, b/2], \quad t \in [0, T]:$$

$$\frac{\partial \Gamma(y, t)}{\partial t} + l_0 \gamma(X(t, t), y) = 0 \tag{23}$$

$$\Gamma(y, t) = -4\pi a(m + q\Omega) + 4\pi a W_{\mathrm{i}}^{\mathrm{QS}}(y, t), \tag{24}$$

where the quasi-steady induced velocity $W_{\mathrm{i}}^{\mathrm{QS}}$ is obtained from an evaluation of (22) and where $\gamma_x(\xi, \eta)$ and $\gamma_y(\xi, \eta)$ are obtained in the same way as for the unsteady case, as described in Section 4.1.

6. NUMERICAL IMPLEMENTATION

It is now possible to derive a numerical implementation for both the unsteady and quasi-steady lifting-line models evolved in the previous sections. The primary aim of the implementation presented in this paper is to validate the unsteady lifting-line model and compare it with a quasi-steady one; this is why plainness has been favoured. What follows is certainly not the only way for such a numerization, and more sophisticated ones can easily be devised. Therefore this section only presents the main points about the numerical scheme, all the more as it makes use of a rather classical discretization scheme, and emphasis will only be laid on the particularities induced by the approach.

First, a linearized framework has been selected; this supposes that the wing's small-amplitude motion is not very different from a rectilinear uniform translation along the x-axis, with speed l_0, so that the wake will be considered as remaining in the plane (O, x, y) and convected relatively to the lifting-line with the average speed l_0.

The following discretization bases have been adopted.

1. The lifting-line is approximated by N segments along the span, possibly different in size.
2. The time interval $[0, T]$ is divided into constant-amplitude time steps Δt.
3. The main unknown of the problem, $\Gamma(y, t)$, is approximated by a step function on each discretization interval in y and t:

$$y \in [y_j, y_{j+1}], \quad t \in [t_k, t_{k+1}] : \quad \Gamma(y, t) \approx \Gamma_{jk},$$

this, in a very classical manner, corrresponding to constant doublet panels on the wake. Consequently, the 3D wake is approximated by a classical vortex filament lattice (see Figure 4), composed of closed rectangular vortex elements with strength Γ_{jk}, with dimension Δy in the span direction and $\Delta x = l_0 \Delta t$ in the streamwise direction.

At each time step the linear equations obtained from the discretization of the system (16), (18) are written at a finite number of collocation points, which are the middles of the segments approximating the lifting-line.

Numerical tests have shown that the X'-value which splits up the 2D wake, as appearing in relation (18), may be taken as the order of the chord. As a matter of fact, it has been chosen as $X' - 2a = \Delta x = l_0 \Delta t$, which corresponds to the part of the 2D wake shed during the current time step (other choices are certainly suitable and this one seems to slightly violate the hypothesis $X' \gg a$, but the results presented later on do not seem to illegitimate it). As a consequence, the integral in (18)

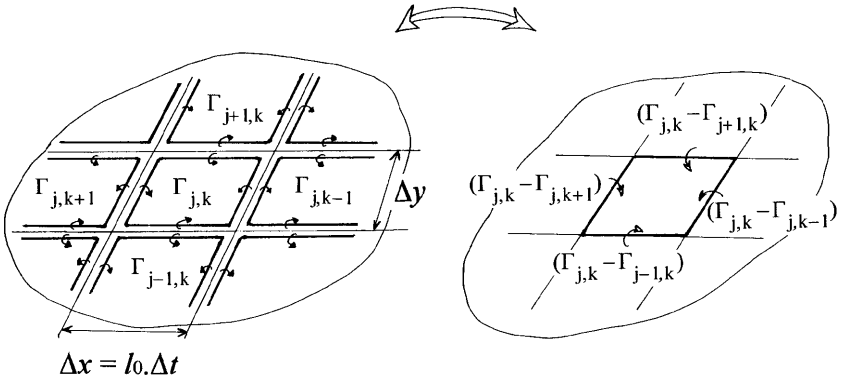

Figure 4. Unsteady three-dimensional wake discretization

refers to the interval $[2a, X']$ and thus to the current time step; the vortex density $\gamma(\chi, y)$ in this integral is approximated assuming a linear variation with respect to χ on the interval $\Delta x = l_0 \Delta t$ (another discrete approximation for $\gamma(\chi, y)$, a constant value for example, is conceivable, but would be less precise for a given time step value).

The expression for $W_i(y, t)$ in relation (20) involves the induced velocity $w_{out}(y, t)$, as defined by (5), on the lifting-line by the 3D unsteady wake, which is approximated in the discrete scheme by the vortex lattice mentioned above. This discretization of the wake presents the advantage that it allows a straight approximation of the finite part of the integral in Hadamard's sense in (5). The fact is that in the case of a straight lifting-line the finite part in Hadamard's sense has to be considered because of the logarithmic singularity which comes from the densities $\gamma_x(\xi, \eta)$ and $\gamma_y(\xi, \eta)$; particularly, in the case of an unswept lifting-line this singularity only comes from $\gamma_y(\xi, \eta)$ (no finite part has to be considered for steady flows, as in this case, $\gamma_y(\xi, \eta) = 0$, and the integral has to be evaluated as a principal value Cauchy-type integral). After having identified the infinite part of an integral, the evaluation of its finite part in Hadamard's sense consists of removing this infinite part through a limiting process. Therefore, as the wake's discrete scheme concentrates vorticity in filaments along the edges of the panels, there is no distributed vortex density, and the logarithmic singular behaviour, especially locally on the lifting-line's collocation points, has been removed. This is why it can be assumed that a vortex lattice discretization of the wake performs a discrete evaluation of the finite part of the integral defining $w_{out}(y, t)$, which can easily be computed using the classical Biot–Savart law applied to the vortex filaments constituting the lattice.

The evaluation of the second term of $W_i(y, t)$ in (20) requires some comments. It involves the two-dimensional wake corresponding to the outer domain O_{wi}, or more precisely, the part extending between the lifting-line and x', i.e. the interval $[0, x']$. The same choice as for the integral in (18) will be made, and it will be considered in the 2D wake shed during the current time step, so that $x' = \Delta x = l_0 \Delta t$. This integral has also to be taken as a finite part in Hadamard's sense; moreover, this term combines with $w_{out}(y, t)$ in the expression of $W_i(y, t)$ and thus requires the same level of discretization. These are the reasons why its evaluation will call for the 2D equivalent of the vortex lattice, i.e. a point vortex approximation of the 2D wake. Furthermore, the vorticity distribution of this 2D wake, as mentioned in Section 4.1, corresponds to the local value of the spanwise vorticity of the 3D wake; thus, following the same process in the discrete scheme, this contribution is evaluated through the velocity induced by a system of 2D vortices whose intensities and streamwise locations are identical to those of the corresponding filaments of the vortex lattice. Finally, as only the current time step is involved, this system reduces to one 2D vortex located at a distance $\Delta x = l_0 \Delta t$ from the lifting-line, and whose intensity is equal to that of the filament of the vortex lattice located at the same distance (see Figure 5).

A time-marching computation algorithm is then adopted. This means that at computation time $t_n = n\Delta t$ the unknowns of the problem are the values Γ_{jn} for $j = 1, \ldots, N$, as the values Γ_{jk}, corresponding to $t_k = k\Delta t$ with $k < n$, have been computed at the previous time steps.

Once their discretization has been carried out according to the principles described above in this section, equations (16) and (18) lead, at computation time t_n, to a linear set of N equations related to the N unknowns Γ_{jn}, which may be formally written for each collocation point y_m as

$$m = 1, \ldots, N: \quad \sum_{j=1}^{N} \alpha_j(y_m)\Gamma_{jn} = 4\pi a(m(t_n) + q(t_n)\Omega) + \sum_{j=1}^{N} \sum_{k=1}^{n-1} \beta_{jk}\Gamma_{jk}, \tag{25}$$

where a, m, q and Ω may vary with y, as stated earlier, and so have different values according to y_m.

This system is solved numerically using a classical linear system resolution method. Then a Δt shift in the computation time values allows us to proceed with the next time step.

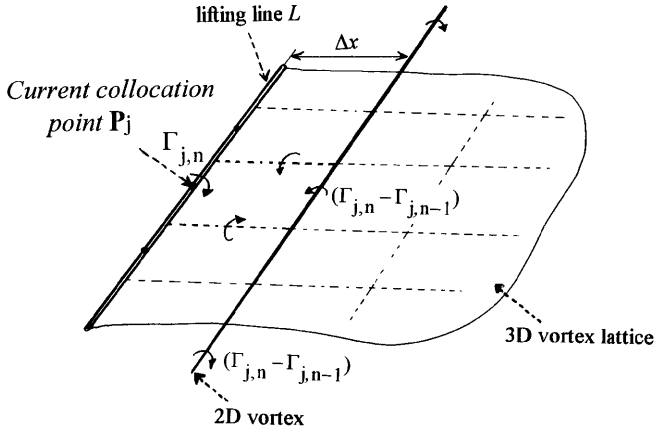

Figure 5. Discrete unsteady induced velocity scheme

The same algorithm and discretization process have been applied to the quasi-steady model described above. Particularly, $\Gamma(y, t)$ and the 3D wake are approximated in the same way, and equation (24) is discretized on the same basis as equation (18) of the unsteady model. It is, however, simpler, as in the quasi-steady case the 2D model does not include any unsteady wake, and the induced velocity $W_i^{QS}(y, t)$ is nothing else than $w_{out}(y, t)$, whose discretization is described above.

Thus it may be pointed out that the unsteady lifting-line model is algorithmically identical to and numerically only slightly different from the quasi-steady one. Consequently, switching from a quasi-steady to an unsteady model induces only a small additional programming effort and, for given lifting-line discretization and time step values, only a slight increase in computation run time, as most of it can be attributed to the computation of $w_{out}(y, t)$ that the two models share in common.

7. SOME NUMERICAL RESULTS

The two models described above, which from now on will be referred to as the QS (quasi-steady) and ULL (unsteady lifting-line) models, have been applied to three different unsteady wing motions:

(a) an instantaneous gust entry for a flat wing initially at incidence 0° and corresponding to a geometrical incidence of 5°
(b) two vertical sinusoidal heave oscillations with reduced periods $\tilde{T} = UT/\bar{c} = 20$ and 60 (where T is the motion period and $\bar{c} = b/AR$ is the mean wing chord) and with amplitude $A = \pm 0.087UT$.

The first one is a very classical, and critical, unsteady aerodynamics benchmark, for which results are available (see e.g. References 16 and 21). The other two are simple periodic movements, and the chosen reduced periods are representative of the working conditions of respectively the foot and the tip of a helicopter rotor blade. These are clearly low-frequency motions in the sense of Section 2 and fall within the above-presented ULL model's domain of application.

Unless noted otherwise, the considered wing is rectangular, with aspect ratio $AR = 10$.

The time evolutions are presented as a function of the dimensionless time $\tilde{t} = Ut/\bar{c}$, which in fact coincides with the number of mean chords $\bar{c}$ travelled during the physical time and is a very useful dimensionless time for unsteady inviscid problems. The time steps are non-dimensionalized in the same way: $\Delta\tilde{t} = U\Delta t/\bar{c}$. The computations for the two heave oscillations have been performed on

three motion periods and the results are presented for the first half of the third one, as the movement is symmetrical; these results can thus be considered as periodically established.

For both models the computation run times ranged from a few seconds to a few minutes on a 486DX personal computer.

7.1. Quasi-steady model

The first three figures concern the quasi-steady model. Figure 6–8 show the time evolution of the non-dimensional circulation $\tilde{\Gamma}(y,\tilde{t}) = \Gamma(y,\tilde{t})/U\bar{c}$ at the span station $y/b = 0{\cdot}275$ for different reduced time step values $\Delta\tilde{t}$ for the three wing motions presented above.

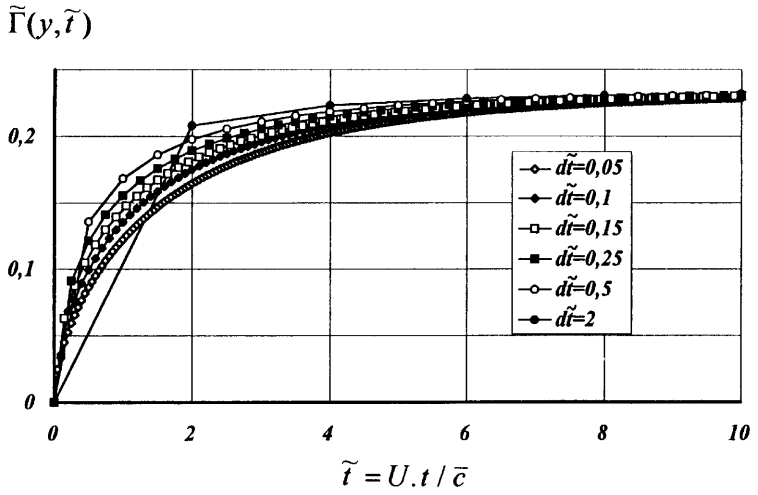

Figure 6. Quasi-steady model—instantaneous gust entry: $\tilde{\Gamma}(y,\tilde{t})$ at span station $y/b = 0{\cdot}275$ for different reduced time step values $\Delta\tilde{t}$

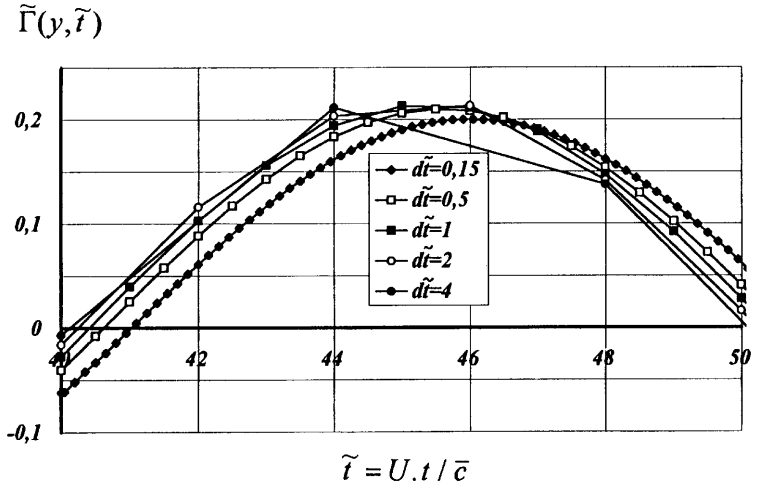

Figure 7. Quasi-steady model—heave oscillation with $\tilde{T} = 20 : \tilde{\Gamma}(y,\tilde{t})$ at span station $y/b = 0{\cdot}275$ for different reduced time step values $\Delta\tilde{t}$ (first half of third period)

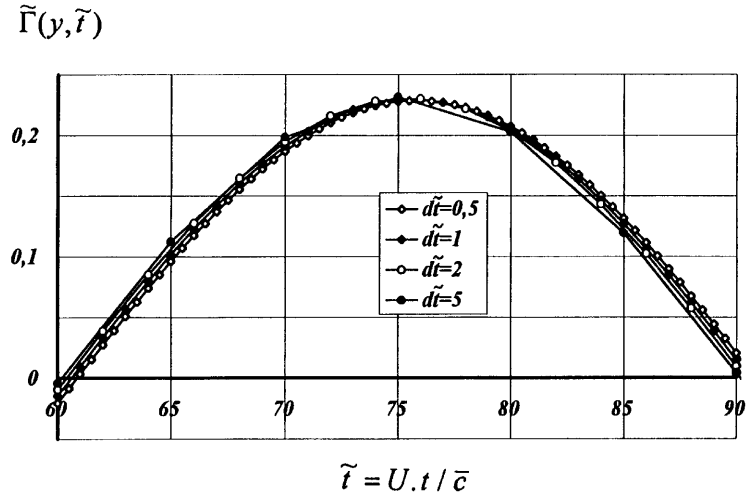

Figure 8. Quasi-steady model—heave oscillation with $\tilde{T} = 60$: $\tilde{\Gamma}(y, \tilde{t})$ at span station $y/b = 0{\cdot}275$ for different reduced time step values $\Delta\tilde{t}$ (first half of third period)

These figures clearly show the time consistency problem to which the QS model is subjected. Actually, a numerical scheme is said to be consistent relative to the time discretization if the solution it produces tends asymptotically towards the solution of the continuous (non-discretized) problem when the time step tends towards zero. Now, and even if the corresponding actual continuous solutions are not explicitly known, it is easy to notice that the solutions obtained in all three cases drift in phase and amplitude without tending towards any tangible limit when the time step decreases, and this is all the more obvious since the unsteadiness is important. This non-consistency can obviously be attributed to the fact that the QS model, based on a steady-type formulation, is only valid in the limiting case of very low frequencies and should not be applied outside this range. Anecdotally, numerical tests have shown that the QS model solutions, in all cases, coincide with reference solutions (unsteady lifting-line model and others) for a reduced time step of about 0·16 chord.

7.2. Unsteady lifting-line model

The next five figures concern the unsteady lifting-line model.

Figure 9 illustrates the model convergence in relation to the number of discrete segments on the span ($\tilde{\Gamma}(y, \tilde{t})$ approximate solution for impulsive gust entry at $\tilde{t} = 10$ chords, which should be very close to the steady state solution, for 10, 20 and 40 segments on the span), compared with the corresponding 3D steady solution (the same wing with a steady 5° angle of attack) obtained with a classical Glauert–Carafoli method.

Figures 10–12 exhibit the evolution of $\tilde{\Gamma}(y, \tilde{t})$ at the span station $y/b = 0{\cdot}275$ for different reduced time step values for the same three wing motions. These figures have to be compared respectively with Figures 6–8 of Section 7.1. In contrast with the QS model, the time consistency of the ULL model is quite clear, even in the most severe case of impulsive motion. It can be noticed in that case that the first computed value is obviously underestimated; this may certainly be attributed to the numerical scheme, and the first computation step probably deserves a more refined numerical scheme. Nevertheless, it is particularly noticeable that a time step as large as one chord already

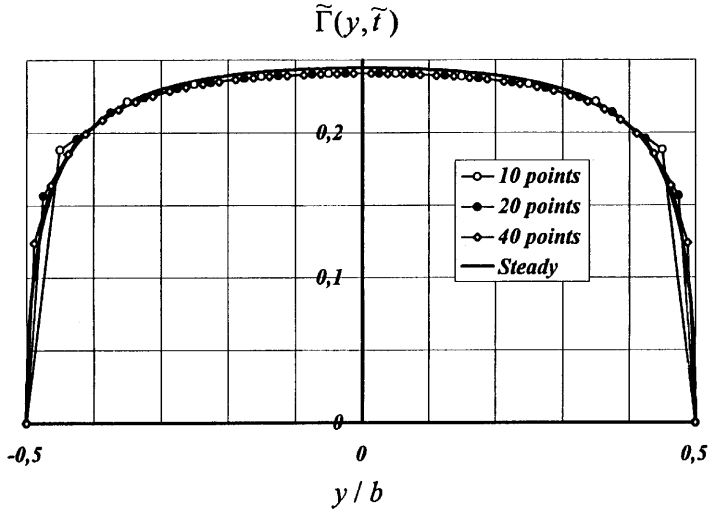

Figure 9. Unsteady lifting-line model convergence—instantaneous gust entry: effect of number of discrete segments on span (10, 20 and 40 segments) on $\tilde{\Gamma}(y, \tilde{t})$ for impulsive incidence setting at $\tilde{t} = 10$ chords; comparison with a 3D steady solution

provides a rather satisfactory solution. The case of the translatory oscillation is even more interesting, as quite large time step values ($\Delta\tilde{t} = 4$ chords for $\tilde{T} = 20$ chords and $\Delta\tilde{t} = 10$ chords for $\tilde{T} = 60$ chords) lead to solutions very near to those obtained with small time step values, which may be considered as converged.

Figure 13 compares the time evolution of the ratio of the wing's instantaneous lift to its final steady lift for impulsive gust entry and for different aspect ratios ($AR = 6, 10$ and ∞ (two-dimensional case)). It may be pointed out that the ULL model behaves quite satisfactorily relative to the aspect ratio, as it shows the classical result that the lift response of the wing is all the faster since the aspect ratio is small. This figure also compares this evolution with a result of Jones[21] for an elliptic wing

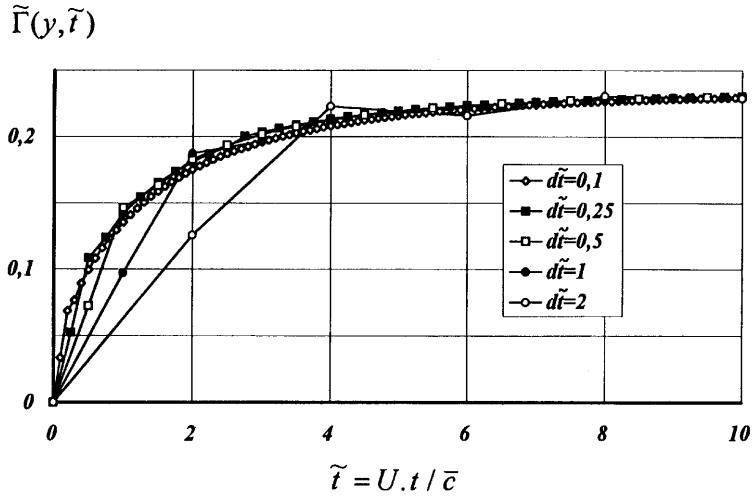

Figure 10. Unsteady lifting-line model—instantaneous gust entry: $\tilde{\Gamma}(y, \tilde{t})$ at span station $y/b = 0{\cdot}275$ for different reduced time step values $\Delta\tilde{t}$

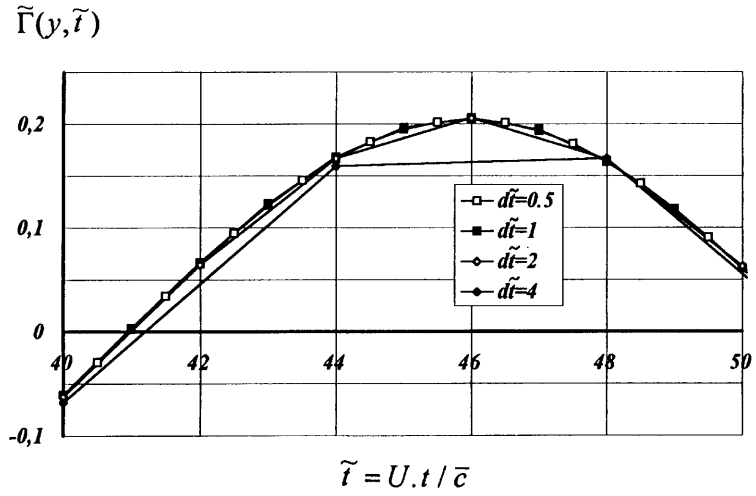

Figure 11. Unsteady lifting-line model—heave oscillation with $\tilde{T} = 20$: $\tilde{\Gamma}(y, \tilde{t})$ at span station $y/b = 0{\cdot}275$ for different reduced time step values $\Delta\tilde{t}$ (first half of third period)

with aspect ratio $AR = 6$. It can be noticed that the ULL model results for the same aspect ratio convincingly coincide and the slight discrepancy between these two results can certainly be imputed to the plan-form difference (a rectangular wing versus an elliptic one).

In conclusion of this section, it may be considered that the results presented above validate the principles of the unsteady lifting-line approach and its numerical implementation. In fact, it is clear that this validation has to be more thoroughly carried out, but this comes up against the problem of finding reliable validation benchmarks. Nevertheless, it can be noted from the above numerical study that the ULL model is time-consistent and that the numerical results it produces may be considered as

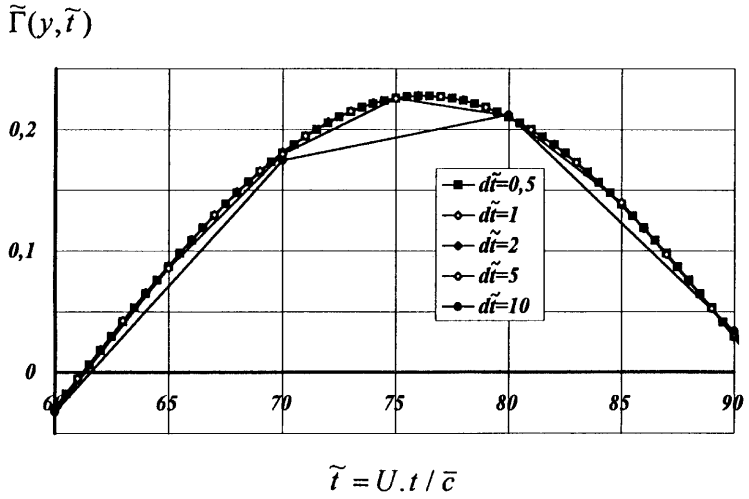

Figure 12. Unsteady lifting-line model—heave oscillation with $\tilde{T} = 60$: $\tilde{\Gamma}(y, \tilde{t})$ at span station $y/b = 0{\cdot}275$ for different reduced time step values $\Delta\tilde{t}$ (first half of third period)

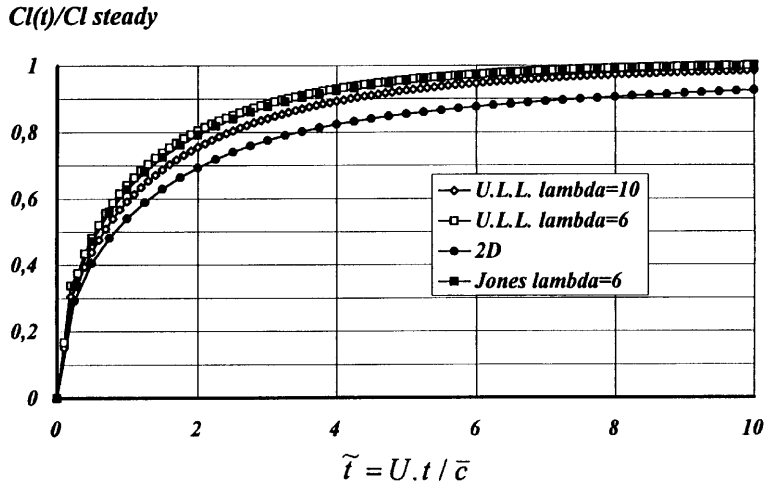

Figure 13. Unsteady lifting-line—instantaneous gust entry: time evolution of ratio of instantaneous lift to final steady lift for $AR = 6$, 10 and ∞ (2D); comparison with a result of Jones[21]

converged for quite large time steps. Furthermore, the comparisons with the results of R. T. Jones provide us with a quantitative validation.

8. CONCLUSIONS

The work presented in this paper allows us to put forward the basis for a time-marching unsteady lifting-line approach and the ensuing numerical implementation. It actually uses the same process and algorithm as the quasi-steady one, which is in fact Prandtl's approach for steady flows applied to unsteady cases.

This approach consists of searching for the solution to the first-order unsteady outer problem, i.e. the time evolution of the spanwise circulation distribution along the lifting-line, through the resolution for each span section of a 2D unsteady problem, which takes into account the three-dimensional aspect of the problem through an unsteady induced velocity on the lifting-line. The theoretical developments based on the MAE technique allows us to justify this approach and, in this context, to clarify the concept of an unsteady induced velocity on the lifting-line.

A simple linearized time-marching numerical implementation has been devised for the ULL model as well as for the QS one. This allows us to state that the QS model numerization cannot be considered as time-consistent, whereas the ULL one is; furthermore, the ULL model's numerical implementation accepts large computation time steps, which should guarantee significant computing time savings in engineering applications.

At present, amongst all the improvements that can be brought to this basic model, two are in progress that deals with topics which do not bring any new theoretical problems; these are the extension of the formulation to swept and curved wings, and the introduction of a free vortex wake instead of a linearized one.

REFERENCES

1. M. Van Dyke, *Perturbation Methods in Fluid Mechanics*, Academic, New York, 1964.
2. H. Ashley and J. Landhal, *Aerodynamics of Wings and Bodies*, Addison-Wesley, Reading, MA, 1965.
3. K. O. Friedrichs, *Special Topics in Fluid Dynamics*, Gordon and Breach, New York, 1966.

4. E. C. James, 'Lifting line theory for an unsteady wing as a singular perturbation problem', *J. Fluid Mech.*, **70**, 753–771 (1975).
5. J. Van Holten, 'Some notes on unsteady lifting line theory', *J. Fluid Mech.*, **77**, 561–579 (1977).
6. H. K. Cheng, 'On lifting line theory in unsteady aerodynamics', *USCAE Department of Aerospace Engineering Rep. 133*, 1975.
7. H. K. Cheng, 'Lifting line theory of oblique wings', *AIAA J.*, **16**, 1211–1223 (1978).
8. H. K. Cheng and L. E. Murillo, 'Lunate-tail swimming propulsion as a problem of curved lifting-line in unsteady flow', *J. Fluid Mech.*, **143**, 325–350 (1984).
9. A. R. Ahmadi and S. E. Widnall, 'Unsteady lifting-line theory as a singular perturbation problem', *J. Fluid Mech.*, **153**, 59–81 (1985).
10. J. P. Guiraud and G. Slama, 'Sur la théorie asymptotique de la ligne portante en régime incompressible oscillatoire', *Rech. Aérosp.*, **1**, 1–6 (1981).
11. J. L. Guermond, 'A generalised lifting-line theory for curved and swept wings', *J. Fluid Mech.*, **211**, 497–513 (1990).
12. A Sellier, 'Une théorie unifiée de la ligne portante', *Thesis Dissertation*, Paris VI University, 1990.
13. J. L. Guermond and A. Sellier, 'A unified unsteady lifting-line theory', *J. Fluid Mech.*, **229**, 427–451 (1991).
14. W. G. Bousman, C. Young, N. Gilbert, F. Toulmay, W. Johnson and M. J. Riley, 'Correlation of Puma airloads-lifting line and wake calculation', *15th Eur. Rotorcraft Forum*, Amsterdam, September 1989.
15. B. Michea, 'Etude des sillages de rotors d'hélicoptères en vol d'avancement et de leur influence sur les performances du rotor', *Thesis Dissertation*, Paris VI University, 1992.
16. R. L. Bisplinghoff, H. Ashley and R. L. Halman, *Aeroelasticity*, Addison-Wesley, Reading, MA, 1955.
17. Th. Von Karman and W. R. Sears, 'Airfoil theory for non uniform motion', *J. Aeronaut. Sci.*, **5**, 379–390 (1938).
18. W. R. Sears, 'Some aspects of a non-stationary airfoil theory and its practical application', *J. Aeronaut. Sci.*, **8**, 104–108 (1941).
19. G. Couchet, *Les Profils en Aérodynamique Instationnaire et la Condition de Joukowski*, Librairie Scientifique et Technique Albert Blanchard, Paris, 1976.
20. Ph. Devinant, 'Numérisation fine d'écoulements fortement instationnaires autour de profils arbitraires', *Thesis Dissertation*, Orléans University, 1982.
21. R. T. Jones, 'The unsteady lift of a wing of finite aspect ratio', *NACA Rep. 681*, 1939, pp. 31–38.

